LETTER

doi:10.1038/nature10798

Dysfunction of lipid sensor GPR120 leads to obesity in both mouse and human

Atsuhiko Ichimura[1]*, Akira Hirasawa[1]*, Odile Poulain-Godefroy[2,3]*, Amélie Bonnefond[2,3]*, Takafumi Hara[1], Loïc Yengo[2,3], Ikuo Kimura[1], Audrey Leloire[2,3], Ning Liu[1], Keiko Iida[1], Hélène Choquet[2,3], Philippe Besnard[4], Cécile Lecoeur[2,3], Sidonie Vivequin[2,3], Kumiko Ayukawa[1], Masato Takeuchi[1], Kentaro Ozawa[1], Maithé Tauber[5], Claudio Maffeis[6,7], Anita Morandi[2,3,6], Raffaella Buzzetti[8], Paul Elliott[9], Anneli Pouta[10,11], Marjo-Riitta Jarvelin[9,10,12], Antje Körner[13], Wieland Kiess[13], Marie Pigeyre[14,15], Roberto Caiazzo[14,16], Wim Van Hul[17], Luc Van Gaal[18], Fritz Horber[19], Beverley Balkau[20,21], Claire Lévy-Marchal[22], Konstantinos Rouskas[2,3,23], Anastasia Kouvatsi[23], Johannes Hebebrand[24], Anke Hinney[24], Andre Scherag[25], François Pattou[14,16], David Meyre[2,3,26], Taka-aki Koshimizu[27], Isabelle Wolowczuk[2,3], Gozoh Tsujimoto[1] & Philippe Froguel[2,3,28]

Free fatty acids provide an important energy source as nutrients, and act as signalling molecules in various cellular processes[1–4]. Several G-protein-coupled receptors have been identified as free-fatty-acid receptors important in physiology as well as in several diseases[3,5–13]. GPR120 (also known as O3FAR1) functions as a receptor for unsaturated long-chain free fatty acids and has a critical role in various physiological homeostasis mechanisms such as adipogenesis, regulation of appetite and food preference[5,6,14–16]. Here we show that GPR120-deficient mice fed a high-fat diet develop obesity, glucose intolerance and fatty liver with decreased adipocyte differentiation and lipogenesis and enhanced hepatic lipogenesis. Insulin resistance in such mice is associated with reduced insulin signalling and enhanced inflammation in adipose tissue. In human, we show that *GPR120* expression in adipose tissue is significantly higher in obese individuals than in lean controls. *GPR120* exon sequencing in obese subjects reveals a deleterious non-synonymous mutation (p.R270H) that inhibits GPR120 signalling activity. Furthermore, the p.R270H variant increases the risk of obesity in European populations. Overall, this study demonstrates that the lipid sensor GPR120 has a key role in sensing dietary fat and, therefore, in the control of energy balance in both humans and rodents.

To investigate the role of GPR120 in metabolism, we examined GPR120-deficient mice (Supplementary Fig. 1) with respect to lipogenesis, glucose and energy homeostasis. On a normal diet containing 13% fat, the body weight was similar in both GPR120-deficient and wild-type mice. However, when 5-week-old GPR120-deficient mice were fed a high-fat diet (HFD) containing 60% fat, their body weight increase was ~10% higher than that of wild-type mice on a HFD (Fig. 1a). The difference in HFD-induced body weight gain between wild-type and GPR120-deficient mice was marked at ~8–10 weeks old and reached a plateau at 13 weeks old. To assess energy expenditure and substrate utilization, we next performed indirect calorimetry on wild-type and mutant mice on a HFD at 9–10 weeks old (Fig. 1b) and 15–16 weeks old (Supplementary Fig. 2a). The young GPR120-deficient mice showed decreased energy expenditure compared with the young wild-type mice, particularly during the light/inactive phase (Fig. 1b, left), whereas older mutant and wild-type mice showed no such a difference (Supplementary Fig. 2a, left). The difference in energy expenditure between GPR120-deficient and wild-type mice was observed only in the light phase, indicating that the lack of the GPR120 receptor primarily affects basal metabolism, especially in young mice. The decreased energy expenditure might explain the difference we found in body weight gain between HFD-fed wild-type and mutant young mice. The lower values of respiratory quotient in mutant mice could be due to insufficient glucose utility, probably as a result of the decreased insulin sensitivity. In all experiments, both groups of mice showed similar levels of locomotor activity (data not shown).

White adipose tissue (WAT) and liver were substantially heavier in HFD-fed GPR120-deficient mice (Supplementary Fig. 2b). Plasma low- and high-density lipoprotein cholesterol levels were significantly higher in HFD-fed GPR120-deficient mice, and serum alanine aminotransferase levels were substantially increased, indicating abnormal cholesterol metabolism and liver function (Supplementary Table 1). Microcomputed tomography scanning revealed that 16-week-old GPR120-deficient mice stored much more fat than did wild type (Fig. 1c). A significant increase in adipocyte size in both epididymal (Fig. 1d) and subcutaneous (Supplementary Fig. 2c) fat was observed in GPR120-deficient mice. Furthermore, the expression of macrophage marker genes (*Cd11b* (*Itgam*), *Cd68* and *F4/80* (*Emr1*)) and the number of F4/80-positive cells were markedly enhanced in epididymal tissue from HFD-fed GPR120-deficient mice (Fig. 1e, f). Moreover, these mice showed liver steatosis and hepatic triglyceride content was markedly increased (Fig. 1g). Overall, HFD-induced obesity and liver fattiness were more severe in GPR120-deficient mice than in wild type.

[1]Department of Genomic Drug Discovery Science, Graduate School of Pharmaceutical Sciences, Kyoto University, 46-29 Yoshida Shimoadachi-cho, Sakyo-ku, Kyoto 606-8501, Japan. [2]Centre National de la Recherche Scientifique (CNRS)-Unité mixte de recherche (UMR) 8199, Lille Pasteur Institute, Lille 59000, France. [3]Lille Nord de France University, Lille 59000, France. [4]Institut National de la Santé et de la Recherche Médicale (Inserm)-UMR U866, Physiologie de la Nutrition, Bourgogne University, AgroSup Dijon, Dijon 21078, France. [5]Inserm-U563, Children's Hospital, Centre Hospitalier Universitaire, Toulouse 31000, France. [6]Regional Centre for Juvenile Diabetes, Obesity and Clinical Nutrition, Verona 37134, Italy. [7]Department of Mother and Child, Biology-Genetics, Section of Paediatrics, University of Verona, Verona 37134, Italy. [8]Department of Clinical Sciences, La Sapienza University, Rome 00161, Italy. [9]Medical Research Council-HPA Centre for Environment and Health, Department of Epidemiology and Biostatistics, School of Public Health, St Mary's campus, Imperial College London, London W2 1PG, UK. [10]National Public Health Institute, Biocenter Oulu, University of Oulu, Oulu 90220, Finland. [11]Institute of Clinical Medicine/Obstetrics and Gynecology, University of Oulu, Oulu 90220, Finland. [12]Institute of Health Sciences, University of Oulu, Oulu 90220, Finland. [13]Center for Pediatric Research, Department of Women's & Child Health, University of Leipzig, Leipzig 04317, Germany. [14]Inserm-U859, Lille Nord de France University, Lille 59000, France. [15]Lille University Hospital, Nutrition, Lille 59000, France. [16]Lille University Hospital, Endocrine Surgery, Lille 59000, France. [17]Department of Medical Genetics, University of Antwerp, Antwerp 2610, Belgium. [18]Department of Endocrinology, Antwerp University Hospital, Antwerp 2650, Belgium. [19]Department of Surgery and Internal Medicine, Clinic Lindberg, Medical Department, Winterthur 8400, and University of Berne, Berne 3011, Switzerland. [20]Inserm-U780, Centre for research in Epidemiology and Population Health (CRESP), Villejuif 94800, France. [21]Paris-Sud 11 University, Orsay 91405, France. [22]Inserm-U690, Robert Debré hospital, Paris 75935, France. [23]Department of Genetics, Development and Molecular Biology, School of Biology, Aristotle University of Thessaloniki, Thessaloniki 541 24, Greece. [24]Department of Child and Adolescent Psychiatry, University of Duisburg-Essen, Essen 45147, Germany. [25]Institute for Medical Informatics, Biometry and Epidemiology, University of Duisburg-Essen, Essen 45122, Germany. [26]McMaster University, Hamilton, Ontario L8S 4L8, Canada. [27]Department of Pharmacology, Division of Molecular Pharmacology, Jichi Medical University, Tochigi 329-0498, Japan. [28]Department of Genomics of Common Disease, School of Public Health, Imperial College London, Hammersmith Hospital, London W12 0NN, UK.
*These authors contributed equally to this work.

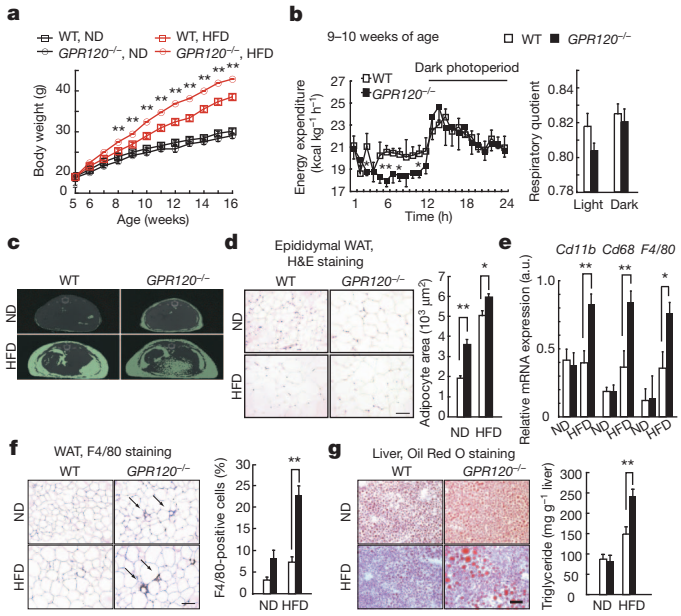

Figure 1 | Obesity, hypertrophic adipocytes, accumulation of pro-inflammatory macrophages and hepatic steatosis in HFD-fed GPR120-deficient mice. **a**, Body weight changes of wild-type (WT) and GPR120-deficient mice fed a normal diet (ND) or a HFD ($n = 36–47$). **b**, Indirect calorimetry in HFD-fed mice. Energy expenditure and respiratory quotient ($n = 4, 5$). **c**, Representative cross-sectional images of wild-type and GPR120-deficient mice subjected to microcomputed tomography analysis of the *in situ* accumulation of fat. Fat depots are demarcated (green) for illustration. **d**, Haematoxylin and eosin (H&E)-stained epididymal WAT and mean area of adipocytes ($n = 6$). Scale bar, 100 μm. **e**, Relative expression of *Cd11b*, *Cd68* and *F4/80* messenger RNA in WAT ($n = 6$). a.u., arbitrary units. **f**, Representative images of epididymal WAT stained with anti-F4/80 antibody (arrows, F4/80-positive cells) and the number of F4/80 cells ($n = 6$). Scale bar, 100 μm. **g**, Oil Red O-stained liver and hepatic triglyceride content after 24hr fasting ($n = 13$). Scale bar, 50 μm. All data represent mean ± s.e.m. $*P < 0.05$ and $**P < 0.01$ versus the corresponding wild-type value.

Obesity-associated insulin resistance was also more severe in GPR120-deficient mice. HFD-fed GPR120-deficient mice showed higher levels of fasting plasma glucose and insulin than did wild type, although these parameters were similar between the two groups on a normal diet (Fig. 2a). HFD-induced insulin resistance, as determined by an insulin tolerance test, was more prominent in GPR120-deficient mice than in wild type (Fig. 2b, left, and Supplementary Fig. 3a, b). A glucose tolerance test further revealed that these mice suffered from impaired glucose metabolism (Fig. 2b, right, and Supplementary Fig. 3a, b). The level of plasma leptin was significantly higher in HFD-fed GPR120-deficient mice than in wild type (Supplementary Fig. 3c). However, there was no significant difference in terms of plasma adiponectin level or food intake between the two groups (Supplementary Fig. 3d, e). HFD-fed GPR120-deficient mice showed a marked increase in the size of islets and KI67 (MKI67)-positive cells, suggesting adaptive enlargement of the β-cell mass in response to insulin resistance[17,18] (Supplementary Fig. 3f, g). Moreover, we observed markedly reduced peripheral insulin sensitivity in tissues from HFD-fed GPR120-deficient mice (Fig. 2c). Insulin was shown to induce the phosphorylation of AKT (AKT1) (on Ser 473) in WAT, liver and skeletal muscle, with similar intensities in wild-type and GPR120-deficient mice on a normal diet (Supplementary Fig. 3h). Consistent with the insulin resistance reported above, HFD-fed GPR120-deficient mice showed loss of insulin-induced AKT phosphorylation in WAT and the liver.

To determine the molecular basis of the metabolic changes in WAT and livers of GPR120-deficient mice, we performed gene expression

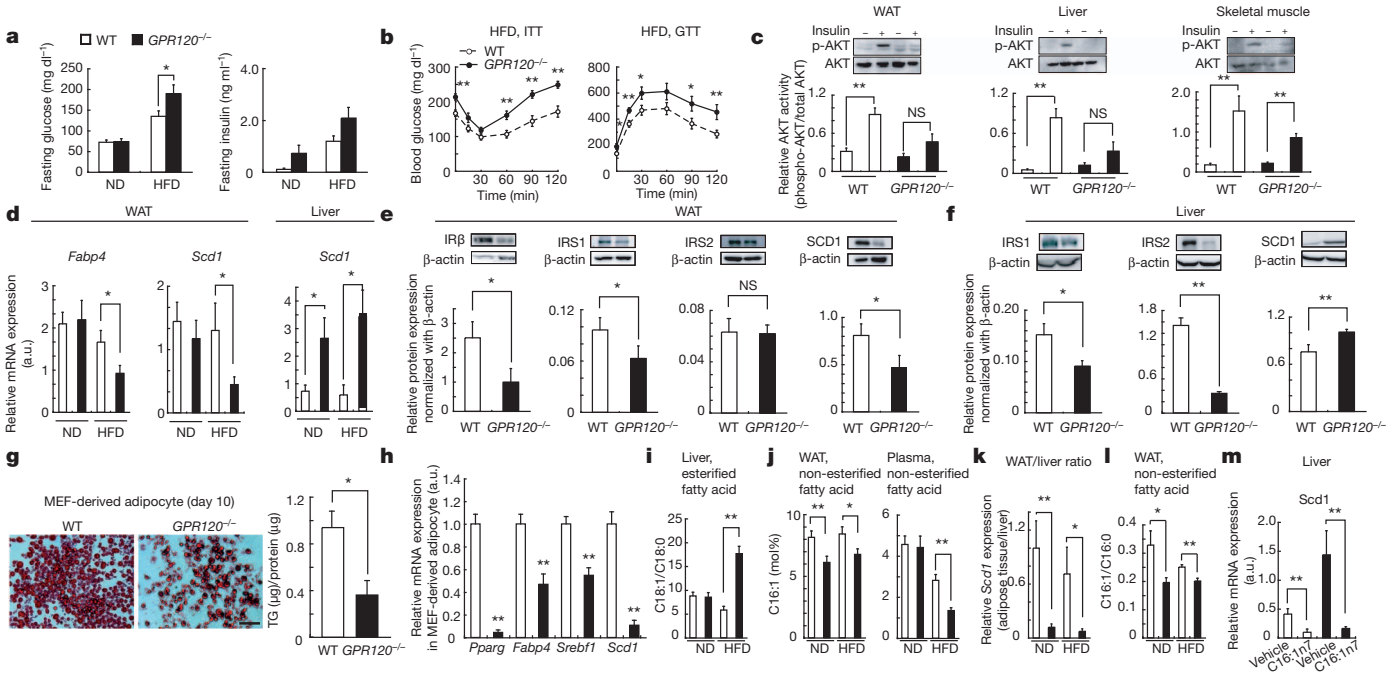

Figure 2 | Impaired glucose metabolism, adipogenesis and lipogenesis in HFD-fed GPR120-deficient mice. **a**, Fasting blood glucose and serum insulin levels ($n = 6–15$). **b**, Plasma glucose during insulin tolerance test (ITT, left) and glucose tolerance test (GTT, right) ($n = 12–14$). **c**, Phosphorylation of AKT (Ser 473) in WAT, liver and skeletal muscle after 24-hr fasting ($n = 6, 7$). NS, not significant. **d**, Relative mRNA expression of *Fabp4* and *Scd1* in WAT or *Scd1* in liver ($n = 6$). **e**, Protein expression of IRβ, IRS1, IRS2, SCD1 and β-actin in WAT. **f**, Protein expression of IRS1, IRS2, SCD1 and β-actin in liver. **g**, Oil Red O-staining and triglyceride (TG) content of mouse embryonic fibroblast (MEF)-derived adipocyte. Scale bar, 50 μm. **h**, Relative mRNA expression in MEF-derived adipocyte ($n = 6$). **i**, The ratio of C18:1 to C18:0 in livers ($n = 6–8$). **j**, Non-esterified C16:1n7 palmitoleate in WAT and plasma ($n = 4–7$). **k**, The ratio of *Scd1* mRNA expression in liver and WAT ($n = 6, 7$). **l**, The ratio of C16:1 to C16:0 in adipose tissues ($n = 6–8$). **m**, Hepatic *Scd1* mRNA expression in mice infused with vehicle or triglyceride:palmitoleate for 6 h ($n = 4, 5$). All data represent mean ± s.e.m. $*P < 0.05$ and $**P < 0.01$ versus the corresponding wild-type value.

analyses. We identified approximately 700 differentially expressed genes in WAT between HFD-fed GPR120-deficient and wild-type mice (Supplementary Fig. 4a). Connectivity mapping of these genes showed that pathways relating to insulin signalling and adipocyte differentiation were depressed, whereas those related to inflammation were enhanced in HFD-fed GPR120-deficient mice (Supplementary Fig. 4b). Quantitative real-time PCR (qRT–PCR) analysis confirmed the downregulation of insulin-signalling-related genes (*Insr*, *Irs1* and *Irs2*), an adipocyte differentiation marker gene (*Fabp4*) and a lipogenesis-related gene (*Scd1*) in the epididymal fat from HFD-fed GPR120-deficient mice (Fig. 2d and Supplementary Fig. 3i). We identified approximately 100 differentially expressed genes in the liver between HFD-fed GPR120-deficient and wild-type mice (Supplementary Fig. 5). Notably, lipogenesis-related genes (*Scd1* and *Me1*) and a fatty acid transporter gene (*Cd36*) were significantly upregulated in livers from GPR120-deficient mice. Quantitative RT–PCR analysis confirmed upregulation of *Scd1* in the liver of GPR120-deficient mice (Fig. 2d).

Western blot analysis further confirmed downregulation of IRβ, IRS1 and SCD1 in adipose tissue of HFD-fed GPR120-deficient mice (Fig. 2e) but downregulation of IRS1 and IRS2 and upregulation of SCD1 in their livers (Fig. 2f). Hence, insulin-signalling-related molecules were downregulated by the lack of GPR120 in both adipose tissue and the liver. However, the expression of SCD1, the rate-limiting enzyme in the biosynthesis of mono-unsaturated fatty acids, was downregulated in adipose tissue but upregulated in liver. Furthermore, the expression of *Scd1* and several adipogenic genes[14,19] (*Pparg*, *Fabp4* and *Srebf1*) was suppressed in mouse-embryonic-fibroblast-derived adipocytes from GPR120-deficient mice, indicating that GPR120 is required for normal adipogenesis, as previously reported in differentiating 3T3-L1 adipocytes depleted of endogenous GPR120 by short interfering RNA[14] (Fig. 2g, h).

To determine the effects of altered lipogenesis on lipid composition in GPR120-deficient mice, we performed lipidomics analysis in WAT, livers and plasma. Significant changes of major lipid clusters were observed (Supplementary Fig. 6). Notably, the hepatic concentration of oleate (C18:1n9c) was significantly higher in HFD-fed GPR120-deficient mice than in wild type. The ratio of C18:1 to C18:0, an indicator of SCD1 enzyme activity[20–23], was markedly enhanced in livers from HFD-fed GPR120-deficient mice relative to wild type (Fig. 2i). Moreover, the levels of C16:1n7 palmitoleate, which has recently been recognized as a lipid hormone[4], in WAT and plasma were significantly lower in HFD-fed GPR120-deficient mice than in wild type (Fig. 2j). In particular, lower levels of C16:1n7 palmitoleate were detected even in WAT of GPR120-deficient mice on a normal diet (Fig. 2j), which seems to be in good agreement with the suppressed *Scd1* expression and the reduced SCD1 desaturation index[20–23] (C16:1/C16:0; Fig. 2k, l). Lipidomics analysis clearly illustrated dysregulated lipogenesis in GPR120-deficient mice, and showed the reduced production of lipid hormone C16:1n7 palmitoleate[4]. To determine whether the enhanced hepatic lipogenesis in GPR120-deficient mice was due to the reduced levels of C16:1n7 palmitoleate, we examined the effect of C16:1n7 palmitoleate treatment on hepatic *Scd1* expression. A 6-h infusion of triglyceride:palmitoleate markedly lowered the enhanced hepatic *Scd1* expression in GPR120-deficient mice (Fig. 2m). The results indicated that the reduced C16:1n7 palmitoleate may explain the systemic metabolic disorders observed in GPR120-deficient mice on a HFD, as palmitoleate has been proposed to be a bioactive lipid by which adipose tissue communicates with distant organs (such as liver) and regulates systemic metabolic homeostasis[4]. This study shows that dysfunction of GPR120 can be an underlying mechanism for diet-associated obesity and obesity-related metabolic disorders in mouse.

The mouse data prompted us to assess the potential contribution of GPR120 to the development of obesity and its metabolic complications in humans. First, the expression levels of *GPR120* in both subcutaneous and omental adipose tissues as well as in liver samples were compared between lean and obese subjects. Normoglycaemic obese patients and lean individuals ($n = 14$ in each group) were matched for age and gender (Supplementary Table 2). As previously described[5,14], we confirmed that *GRP120* is barely expressed in liver of either lean or obese subjects (data not shown). By contrast, we found that *GPR120* is well expressed in the adipose tissue of lean individuals (Fig. 3a). In addition, human obesity is significantly associated with an increase in *GPR120* expression in both subcutaneous and omental adipose tissues (1.8-fold increase; $P = 0.0004$ and $P = 0.003$, respectively). We also found that *GPR120* expression in subcutaneous adipose tissue strongly correlates with that in omental adipose tissue (Spearman analysis; $r = 0.570$ and $P = 2.74 \times 10^{-8}$), suggesting a systemic regulation of its expression in humans. Furthermore, we found a positive correlation between *GPR120* expression in both subcutaneous and omental adipose tissues and in subjects' concentrations of plasma low-density lipoproteins (on adjustment for age and sex; $r = 0.247$, $P = 0.0115$ and $r = 0.255$, $P = 0.0118$, respectively).

To investigate the contribution of *GPR120* to human obesity, the four *GPR120* exons were sequenced in 312 French, non-consanguineous, extremely obese children and adults (Supplementary Table 3). We

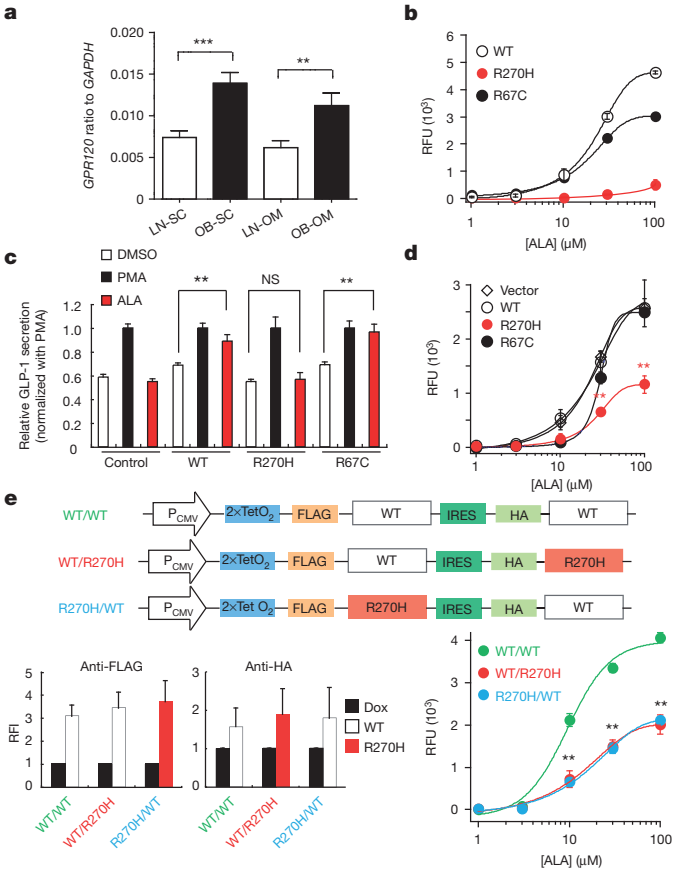

Figure 3 | GPR120 expression in human obese tissue samples, and effect of GPR120 variants on $[Ca^{2+}]_i$ response and GLP-1 secretion. **a**, *GPR120* mRNA levels in human subcutaneous (SC) and omental (OM) adipose tissues of lean (LN; $n = 14$) and obese (OB; $n = 14$) normoglycaemic individuals. Mann–Whitney analysis, $***P = 0.0004$ and $**P = 0.003$. **b**, ALA-induced $[Ca^{2+}]_i$ responses in cells expressing wild-type GPR120 or a p.R67C or p.R270H variant. **c**, ALA-induced GLP-1 secretion in NCI-H716 cells expressing a wild-type GPR120, a p.R67C or a p.R270H receptor. **d**, Effect of transfection with GPR120 variants on ALA-induced $[Ca^{2+}]_i$ response in cells stably expressing wild-type GPR120. **e**, Effect of co-expression of human GPR120 p.R270H variant with wild-type GPR120 on ALA-induced $[Ca^{2+}]_i$ response. Top: schematic diagram of constructs. Bottom: expression of wild type and p.R270H (left), and concentration–$[Ca^{2+}]_i$ response for ALA in cells expressing wild-type/wild-type, wild-type/R270H or R270H/wild-type receptors (right). $**P < 0.01$ versus the corresponding control value. RFI, relative fluorescence intensity; RFU, relative fluorescence unit. All data show mean ± s.e.m.

Table 1 | Identified variants in *GPR120* exons and association between the p.R67C/rs6186610 or p.R270H non-synonymous variant and obesity

	Variant	Nucleotide change	Chr 10 position	MAF_1	MAF_2 (controls, $n = 7{,}654$)	MAF_2 (cases, $n = 6{,}942$)	Adjustment: age and gender		Adjustment: age, gender and geography	
							OR [95% CI]	*P*	OR [95% CI]	*P*
Missense variants	p.R67C/rs6186610	C→T	95,316,666	0.05	0.043	0.055	1.16 [1.02, 1.31]	0.022	1.13 [1.00, 1.28]	0.060
	p.R270H	G→A	95,337,031	0.03	0.013	0.024	1.62 [1.31, 2.00]	8.00×10^{-6}	1.58 [1.28, 1.95]	2.17×10^{-5}
Synonymous variants	p.V38V	G→A	95,316,581	0.0016	—	—	—	—	—	—
	p.S192S	G→A	95,325,846	0.0016	—	—	—	—	—	—
	p.V243V	C→T	95,328,938	0.0016	—	—	—	—	—	—
	p.S264S	G→A	95,337,014	0.0016	—	—	—	—	—	—

Variant position was indicated according to human genome build NCBI36/hg18. Association between p.R67C/rs6186610 or p.R270H variant and obesity was assessed by using a logistic regression adjusted for age and gender or for age, gender and geography, under an additive model. Chr, chromosome; MAF_1, minor allele frequency in sequencing data set ($n = 312$ extremely obese individuals); MAF_2, minor allele frequency in the large obesity case-control genotyping data set; OR, odds ratio; CI, confidence interval.

identified only two non-synonymous variants, R270H (minor allele frequency (MAF), ~3%) and p.R67C/rs6186610 (MAF, ~5%), and four rare synonymous variants (MAF, <1%) (Table 1). The two non-synonymous variants were subsequently genotyped in 6,942 unrelated obese individuals and 7,654 control subjects, all of European origin (Supplementary Table 4). By using a logistic regression model adjusted for age and sex, we found that R270H associated with obesity under an additive model (OR = 1.62 $[1.31, 2.00]_{95\%}$ (odds ratio and 95% confidence interval), $P = 8.00 \times 10^{-6}$; Table 1); whereas we found only a trend for association between p.R67C and obesity (OR = 1.16 $[1.02, 1.31]_{95\%}$, $P = 0.022$; Table 1). It is noteworthy that these results were almost the same after adjusting for geographical origin (Table 1).

We then genotyped the p.R270H variant in 1,109 French pedigrees selected for obesity ($n = 5{,}045$) and in 780 German trios with one obese child ($n = 2{,}340$). We observed a significant over-transmission of the p.R270H low-frequency variant to obese offspring in 117 pedigrees or trios where the p.R270H variant was present (transmission, 62%; $P = 0.009$; Supplementary Table 5). This family-based study excludes a hidden population stratification effect as a cause of spurious association.

We assessed the functional significance of both the p.R67C mutation and the p.R270H mutation *in silico* using several programs: arginine residues at positions 67 and 270 presented a high-evolutionary-conservation pattern among mammals and the two amino-acid substitutions were predicted to be potentially damaging (Supplementary Table 6). To examine the influences of the two non-synonymous variants on GPR120 function *in vitro*, we assessed each receptor ability to mobilize intracellular calcium (concentration, $[Ca^{2+}]_i$) in response to the endogenous agonist α-linolenic acid (ALA). We found that ALA induced $[Ca^{2+}]_i$ responses in T-REx 293 cells expressing either wild-type or p.R67C receptor in a dose-dependent manner, whereas ALA-induced $[Ca^{2+}]_i$ responses in cells expressing p.R270H were significantly lower ($P = 1.6 \times 10^{-5}$) than those in cells expressing wild type at ALA concentrations greater than 10 μM (Fig. 3b). We further examined the functional ability of the mutated receptors to secrete GLP-1 (ZGLP1) from human intestinal NCI-H716 cells, as this cell line lacks *GPR120* expression and it can secrete GLP-1 in a regulated manner[5]. ALA induced secretion of GLP-1 in NCI-H716 cells expressing either wild-type ($P = 0.004$) or p.R67C ($P = 3.2 \times 10^{-5}$) receptor, but not in NCI-H716 cells expressing p.R270H mutant ($P = 0.96$) (Fig. 3c). The transfection efficiencies for the *GPR120* variant receptors were confirmed to be almost the same (data not shown). To examine the effect of the p.R270H variant on the wild-type receptor signalling, we analysed the $[Ca^{2+}]_i$ dose–response curves after the transfection of an empty vector, a wild-type receptor plasmid or a p.R270H-mutated plasmid into T-REx 293 cells expressing wild-type GPR120. The transfection of the p.R270H-mutated plasmid suppressed dose–response curves, and the maximal ALA-induced $[Ca^{2+}]_i$ response was significantly decreased ($P = 0.004$; Fig. 3d).

To assess the effect more quantitatively, we analysed $[Ca^{2+}]_i$ dose–response curves in T-REx 293 cells stably expressing bicistronic wild-type/wild-type, wild-type/p.R270H or p.R270H/wild-type receptors (Fig. 3e, top). Almost equal levels of receptor protein expression in each cell line were confirmed by flow cytometry analysis (Fig. 3e, bottom left). Compared with cells expressing wild-type/wild-type receptor, the $[Ca^{2+}]_i$ dose–response curves obtained in cells expressing either wild-type/p.R270H or p.R270H/wild-type receptor were markedly suppressed, and the maximal ALA-induced $[Ca^{2+}]_i$ response was significantly decreased ($P = 1.2 \times 10^{-5}$; Fig. 3e, bottom right). These findings suggest that the p.R270H variant that is significantly associated with obesity has an inhibitory effect on GPR120. The p.R270H mutant lacks the ability to transduce the signal of long-chain free fatty acids, contrary to the p.R67C mutant, which did not associate with obesity.

To analyse whether being a p.R270H variant carrier may affect *GPR120* expression in the adipose tissue, we quantified *GPR120* expression in samples from both obese p.R270H carriers and obese non-carriers. Two hundred and thirty-eight obese normoglycaemic patients from the Atlas Biologique de l'Obésité Sévère cohort had already been genotyped for the p.R270H variant. Ten subjects heterozygous for the p.R270H variant were matched for age, gender and body mass index with ten non-carrier (wild-type) obese normoglycaemic patients (Supplementary Table 7). The expression of *GPR120* was similar between p.R270H carriers and wild-type subjects, both in subcutaneous and omental adipose tissues (Supplementary Fig. 7a), suggesting that the presence of the functionally deleterious mutation has no primary or secondary effect on gene expression in fat depots. The adipogenesis marker *PPARG*, the lipogenesis-related factor *SCD* and the macrophage marker *CD68* were found similarly well expressed in the adipose tissues of wild-type and p.R270H carrier patients (Supplementary Fig. 7b, c). Nevertheless, the expression of the fatty-acid-binding protein *FABP4* in omental adipose tissue was significantly lower in p.R270H carriers than in wild-type individuals (28% decrease, $P = 0.043$; Supplementary Fig. 7b).

Our results provide convincing evidence that the lipid sensor GPR120 is involved in obesity in both mice and humans. Given the role of GPR120 as a physiologic integrator of the environment (especially the fatty diet), these data provide insight into the molecular mechanisms by which the 'Westernized' diet may contribute to early-onset obesity and associated complications including non-alcoholic steatohepatitis. It also brings some understanding of the metabolic effects of the omega-3 fatty acids, which are often proposed as food supplements. This may open novel avenues of research for drug development in the treatment of obesity, lipid metabolism abnormalities and liver diseases, because receptors that sense free fatty acids represent attractive drug targets.

METHODS SUMMARY

GPR120-deficient mice were generated by deleting *Gpr120* exon 1. All animal procedures and euthanasia were reviewed by the local animal care committee approved by local government authorities. Blood analysis, extraction and detection of mRNA and proteins, and immunohistochemical analysis, were performed following standard protocols as described previously[5,24–26]. Details of antibodies, primers and probes are given in Methods. The level of significance for the difference between data sets was assessed using Student's *t*-test. Analysis of variance followed by Tukey's test was used for multiple comparisons.

In human, *GPR120* expression in liver and in both omental and subcutaneous adipose tissues was assessed by quantitative RT–PCR (Taqman), in lean and obese subjects from the Atlas Biologique de l'Obésité Sévère cohort. The four *GPR120* exons were sequenced in 312 French, extremely obese subjects following a standard Sanger protocol. The two identified non-synonymous variants (p.R270H and p.R67C/rs6186610) were subsequently genotyped in a large European obesity case-control study ($n_{cases} = 6{,}942$, $n_{controls} = 7{,}654$), by high-resolution melting analysis and TaqMan, respectively. The association between obesity status and each variant was assessed using logistic regression adjusted first for age and gender and then for age, gender and geography origin, under an additive model. The consequences of the two identified non-synonymous variants for GPR120 function ($[Ca^{2+}]_i$ response and GLP-1 secretion) were assessed *in vitro*. The human study protocol was approved by the local ethics committee, and participants from all of the studies signed an informed consent form.

Full Methods and any associated references are available in the online version of the paper at www.nature.com/nature.

Received 9 November; accepted 14 December 2011.
Published online 19 February 2012.

1. Nunez, E. A. Biological complexity is under the 'strange attraction' of non-esterified fatty acids. *Prostaglandins Leukot. Essent. Fatty Acids* **57,** 107–110 (1997).
2. Haber, E. P. *et al.* Pleiotropic effects of fatty acids on pancreatic β-cells. *J. Cell. Physiol.* **194,** 1–12 (2003).
3. Itoh, Y. *et al.* Free fatty acids regulate insulin secretion from pancreatic beta cells through GPR40. *Nature* **422,** 173–176 (2003).
4. Cao, H. *et al.* Identification of a lipokine, a lipid hormone linking adipose tissue to systemic metabolism. *Cell* **134,** 933–944 (2008).
5. Hirasawa, A. *et al.* Free fatty acids regulate gut incretin glucagon-like peptide-1 secretion through GPR120. *Nature Med.* **11,** 90–94 (2005).
6. Steneberg, P., Rubins, N., Bartoov-Shifman, R., Walker, M. D. & Edlund, H. The FFA receptor GPR40 links hyperinsulinemia, hepatic steatosis, and impaired glucose homeostasis in mouse. *Cell Metab.* **1,** 245–258 (2005).
7. Wang, J., Wu, X., Simonavicius, N., Tian, H. & Ling, L. Medium-chain fatty acids as ligands for orphan G protein-coupled receptor GPR84. *J. Biol. Chem.* **281,** 34457–34464 (2006).
8. Ichimura, A., Hirasawa, A., Hara, T. & Tsujimoto, G. Free fatty acid receptors act as nutrient sensors to regulate energy homeostasis. *Prostaglandins Other Lipid Mediat.* **89,** 82–88 (2009).
9. Maslowski, K. M. *et al.* Regulation of inflammatory responses by gut microbiota and chemoattractant receptor GPR43. *Nature* **461,** 1282–1286 (2009).
10. Ahmed, K. *et al.* An autocrine lactate loop mediates insulin-dependent inhibition of lipolysis through GPR81. *Cell Metab.* **11,** 311–319 (2010).
11. Oh. Da, Y. *et al.* GPR120 is an omega-3 fatty acid receptor mediating potent anti-inflammatory and insulin-sensitizing effects. *Cell* **142,** 687–698 (2010).
12. Hara, T., Hirasawa, A., Ichimura, A., Kimura, I. & Tsujimoto, G. Free fatty acid receptors FFAR1 and GPR120 as novel therapeutic targets for metabolic disorders. *J. Pharm. Sci.* **100,** 3594–3601 (2011).
13. Kimura, I. *et al.* Short-chain fatty acids and ketones directly regulate sympathetic nervous system via G protein-coupled receptor 41 (GPR41). *Proc. Natl Acad. Sci. USA* **108,** 8030–8035 (2011).
14. Gotoh, C. *et al.* The regulation of adipogenesis through GPR120. *Biochem. Biophys. Res. Commun.* **354,** 591–597 (2007).
15. Tanaka, T. *et al.* Free fatty acids induce cholecystokinin secretion through GPR120. *Naunyn Schmiedebergs Arch. Pharmacol.* **377,** 523–527 (2008).
16. Miyauchi, S. *et al.* Distribution and regulation of protein expression of the free fatty acid receptor GPR120. *Naunyn Schmiedebergs Arch. Pharmacol.* **379,** 427–434 (2009).
17. Kido, Y. *et al.* Tissue-specific insulin resistance in mice with mutations in the insulin receptor, IRS-1, and IRS-2. *J. Clin. Invest.* **105,** 199–205 (2000).
18. Bernal-Mizrachi, E., Wen, W., Stahlhut, S., Welling, C. M. & Permutt, M. A. Islet beta cell expression of constitutively active Akt1/PKB alpha induces striking hypertrophy, hyperplasia, and hyperinsulinemia. *J. Clin. Invest.* **108,** 1631–1638 (2001).
19. Hosooka, T. *et al.* Dok1 mediates high-fat diet-induced adipocyte hypertrophy and obesity through modulation of PPAR-γ phosphorylation. *Nature Med.* **14,** 188–193 (2008).
20. Ntambi, J. M. *et al.* Loss of stearoyl-CoA desaturase-1 function protects mice against adiposity. *Proc. Natl Acad. Sci. USA* **99,** 11482–11486 (2002).
21. Gutierrez-Juarez, R. *et al.* Critical role of stearoyl-CoA desaturase-1 (SCD1) in the onset of diet-induced hepatic insulin resistance. *J. Clin. Invest.* **116,** 1686–1695 (2006).
22. Jeyakumar, S. M. *et al.* Fatty acid desaturation index correlates with body mass and adiposity indices of obesity in Wistar NIN obese mutant rat strains WNIN/Ob and WNIN/GR-Ob. *Nutr. Metab. (Lond.)* **6,** 27 (2009).
23. Brown, J. M. *et al.* Combined therapy of dietary fish oil and stearoyl-CoA desaturase 1 inhibition prevents the metabolic syndrome and atherosclerosis. *Arterioscler. Thromb. Vasc. Biol.* **30,** 24–30 (2010).
24. Ichimura, A., Ruike, Y., Terasawa, K., Shimizu, K. & Tsujimoto, G. MicroRNA-34a inhibits cell proliferation by repressing mitogen-activated protein kinase kinase 1 during megakaryocytic differentiation of K562 cells. *Mol. Pharmacol.* **77,** 1016–1024 (2010).
25. Hara, T. *et al.* Novel selective ligands for free fatty acid receptors GPR120 and GPR40. *Naunyn Schmiedebergs Arch. Pharmacol.* **380,** 247–255 (2009).
26. Sun, Q. *et al.* Structure-activity relationships of GPR120 agonists based on a docking simulation. *Mol. Pharmacol.* **78,** 804–810 (2010).

Supplementary Information is linked to the online version of the paper at www.nature.com/nature.

Acknowledgements We are indebted to all subjects who participated in these studies. In Japan, the study was supported in part by research grants from the Japan Society for the Promotion of Science; the Ministry of Education, Culture, Sports, Science and Technology of Japan; the Japan Science and Technology Agency; and the Funding Program for World-Leading Innovative R&D on Science and Technology (FIRST Program), initiated by the Council for Science and Technology Policy. A.I. is a fellow of the Japan Society for the Promotion of Science. A.B. is a fellow of the EU-funded EUROCHIP consortium. In France, the study was supported by le Conseil Régional Nord Pas de Calais/FEDER and the Agence Nationale de la Recherche (Programme de Recherche en Nutrition et Alimentation, SensoFAT). The Northern Finland Birth Cohort Studies 1986 received financial support from the Academy of Finland, the University Hospital of Oulu (Finland), the University of Oulu (Finland), the European Commission (EURO-BLCS, Framework 5 award QLG1-CT-2000-01643), and the Medical Research Council (G0500539, G0600705, PrevMetSyn/SALVE). We thank the ABOS consortium and the CIC-CCPPRB (Lille CHRU) team for their help in sample handling and clinical data collection. We are grateful to M. Deweirder and F. Allegaert for human DNA bank management.

Author Contributions A.I., A. Hirasawa, O.P.-G. and A.B. are equally contributing first authors. G.T. and P.F. had the ideas for the mouse and human projects, respectively. A.I., A. Hirasawa, A.B., P.F. and G.T. drafted the manuscript. O.P.-G., H.C., D.M. and I.W. edited the manuscript and contributed to discussions. A. Hirasawa and G.T. designed the mouse research. A.I., A. Hirasawa, K.I. and G.T. created *Gpr120*-mutant mice. A.I., A. Hirasawa, A. Körner, T.H., I.K., T.-a.K., K.A., M. Takeuchi, K.O., N.L. and G.T. conducted biochemical and histochemical analyses for the mouse study. A.I. and A. Hirasawa performed bioinformatic analysis for the mouse study. L.Y. and C.L. performed the statistical analyses, and A.B. contributed to statistical analyses for the human study. O.P.-G. and I.W. designed the human expression gene study. A.L. performed the human expression gene study. H.C. and S.V. performed *GPR120* sequencing and variant genotyping, respectively. P.B., M. Tauber, C.M., A.M., R.B., P.E., M.-R.J., W.V.H., L.V.G., F.H., B.B., C.L.-M., K.R., A. Kouvatsi and F.P. contributed to cohort-study samples and researched data.

Author Information Microarray data have been deposited in the NCBI Gene Expression Omnibus under accession number GSE32095. Reprints and permissions information is available at www.nature.com/reprints. The authors declare no competing financial interests. Readers are welcome to comment on the online version of this article at www.nature.com/nature. Correspondence and requests for materials should be addressed to P.F. (p.froguel@imperial.ac.uk) or G.T. (gtsuji@pharm.kyoto-u.ac.jp).

METHODS

Generation and genotyping of GPR120-deficient mice. GPR120-deficient mice on a mixed C57Bl/6/129 background were generated by homologous recombination. Exon 1 of the *Gpr120* gene was replaced with a PGK-neo cassette (Supplementary Fig. 1).

Animals. Mice were housed under a 12-hr light–dark cycle and given regular chow, MF (Oriental Yeast Co.). For HFD studies, 5-week-old male mice were placed on a 58Y1 diet (PMI Nutrition International) for a total period of 11 weeks. The methods used for animal care and experimental procedures were approved by the Animal Care Committee of Kyoto University.

Indirect calorimetry. Twenty-four-hour energy expenditure and respiratory quotient (RQ) were measured by indirect calorimetry, using an open-circuit calorimeter system (MK-5000RQ, Muromachi Kikai Co.). Respiratory quotient is the ratio of carbon dioxide production to oxygen consumption (VO_2). Energy expenditure was calculated as the product of the calorific value of oxygen ($3.815 + 1.232$RQ) and VO_2. Locomotor activity was measured by using an infrared-ray passive sensor system (Supermex, Muromachi Kikai Co.).

Histology and immunohistochemistry. Epididymal adipose and pancreatic tissues were fixed in 10% neutral-buffered formalin, embedded in paraffin, and sectioned at 5 μm. H&E staining was performed using standard techniques. To measure the diameter of adipocytes and the area of pancreatic islets, the diameters of 100 cells from five sections from each group were measured using NIH IMAGE software. More than 10 fields were examined, islet area was traced and total islet area was calculated and expressed as the average score. Liver tissues were embedded in OCT compound (Sakura Finetech) and snap-frozen in liquid nitrogen. Tissue sections were stained with Oil Red O (Sigma-Aldrich) for lipid deposition using standard methods.

Triglyceride content assay. To determine the triglyceride content of liver, tissue was homogenized with 1/2.5/1.25 (vol/vol) 0.5 M acetic acid/methanol/chloroform. The mixture was shaken and 1.25 volumes of chloroform added. The mixture was shaken overnight and then 1.25 volumes of 0.5 M acetic acid added. After centrifugation at 1,500*g* for 10 min, the organic layer was collected, dried and resuspended in 100% isopropyl alcohol. Measurements were conducted using Triglyceride E-test Wako (Wako).

Glucose tolerance and insulin tolerance tests. Glucose tolerance assays were performed on 24-hr-fasted mice. After baseline glucose values were individually established using One Touch Ultra (LifeScan), each mouse was given an intraperitoneal injection of 1.5 mg glucose per gram of body weight. Insulin tolerance was conducted using the same glucometer. After baseline glucose values were established, mice were given human insulin ($0.75\,\mathrm{mU\,g^{-1}}$ intraperitoneal; Sigma-Aldrich). Clearance of plasma glucose was subsequently monitored at 15, 30, 60, 90 and 120 min post-injection.

Immunoblot analysis. For insulin stimulation, 5 U insulin (Sigma-Aldrich) was injected through the inferior vena cava. Five minutes later, samples of liver, skeletal muscle or WAT were dissected and immediately frozen in liquid nitrogen. Immunoblot analysis were performed as described previously[5,24,25]. Anti-IRS1 (Millipore), anti-IRS2 (Millipore), anti-SCD1 (Santa Cruz Biotechnology), anti-IRβ anti-AKT (Cell Signaling Technology), anti-p-AKT (Cell Signaling Technology) and anti-β-actin (Sigma-Aldrich) antibodies were used as the primary antibodies.

Mouse gene expression analysis. Total RNA was extracted from tissue or cells using ISOGEN (Nippon Gene). Quantitative RT–PCR and microarray analysis were performed as described previously[24,26]. Briefly, genome-wide mRNA expression profiles were obtained by microarray analysis with the Affymetrix GeneChip Mouse 430 2.0 Array, according to the manufacturer's instructions. We used the robust multi-array analysis expression measure that represents the log-transformation of intensities (background corrected and normalized) from the GeneChips[27]. Functional associations between differentially expressed genes were analysed using Ingenuity Pathways Analysis (version 4.0, Ingenuity Systems).

Microcomputed tomography scanning. Images were obtained using a microcomputed tomography system (SHIMADZU ClairvivoCT) with a high-resolution flat-panel detector. The maximum resolution of this modality was less than 40 μm. The scanner was assumed to have a cylindrical field of view of 65.3 mm in section view and of 300 mm in transaxial view. The X-ray source was biased at 60 keV with the anode current set to 160 μA. Computed tomography images were analysed with OSIRIX software (http://www.osirix-viewer.com/).

Fatty acid composition of epididymal WAT, liver and plasma. Esterified and non-esterified fatty acid composition was measured by gas chromatography. Briefly, to analyse esterified fatty acid, samples of epididymal adipose tissue (20–25 mg), liver (25–30 mg) and plasma (100 μl) were snap-frozen in liquid nitrogen and homogenized in 4 ml of 0.5 N KOH-methanol. Samples were then boiled at 100 °C for 30 min to hydrolyse. Total lipids in each sample homogenate were then extracted with hexane, followed by trans-esterification of fatty acids using boron trifluoride-methanol at 100 °C for 15 min. Methylated fatty acids were then extracted with hexane and analysed using a GC-2010AF gas chromatograph (SHIMADZU). For the analysis of non-esterified fatty acid, samples of epididymal adipose tissue (10–15 mg), liver (10–15 mg) and plasma (100 μl) were snap-frozen in liquid nitrogen and homogenized in a mixture of 1.2 ml water, 3 ml methanol and 1.5 ml chloroform. Total lipids in each sample homogenate were extracted with a mixture of 1.2 ml of water and 1.2 ml of chloroform, followed by silylation of fatty acids using *N*,O-bis(trimethylsilyl)trifluoroacetamide with 1% trimethylchlorosilane at 100 °C for 60 min. Silylated fatty acids were then extracted with hexane and analysed using a GC-2010AF gas chromatograph (SHIMADZU).

Mouse embryonic fibroblast adipogenesis assay. To prepare MEFs, we minced 13.5-d-post-coital mouse embryos and digested them with trypsin. Cells were collected and cultured in modified Eagle's medium (α-MEM; supplemented with 10% fetal bovine serum (FBS), $50\,\mathrm{U\,ml^{-1}}$ penicillin and $50\,\mathrm{mg\,ml^{-1}}$ streptomycin). We induced confluent MEFs to undergo adipogenic differentiation by incubating them first for 2 d with $10\,\mathrm{\mu g\,ml^{-1}}$ insulin, 250 nM dexamethasone and 0.5 mM isobutylmethylxanthine (Sigma-Aldrich). We measured cellular triglyceride content with Triglyceride E-test Wako (Wako).

Lipid infusion. Intralipid solution with 2 mM triglycerides:palmitoleate was prepared using a previously described protocol[4]. Briefly, lipids were dissolved in a solvent containing 5% glycerol and 0.72% phosphocholine in 0.9% saline and sonicated repeatedly. Lipids stayed in suspension for one week and had to be vortexed well before loading the syringe and tubing to prevent clogging. Before lipid infusion, mice were anaesthetized and an indwelling catheter was inserted in the left internal jugular vein. After overnight fasting, lipids were infused at a rate of $500\,\mathrm{ml\,kg^{-1}\,h^{-1}}$ for 6 h. At the end of the infusion, tissues were collected.

Statistical analysis of the GPR120-deficient mouse study. The level of significance for the difference between data sets was assessed using Student's *t*-test. Analysis of variance followed by Tukey's test was used for multiple comparisons. Data were expressed as mean ± s.e.m. $P < 0.05$ was considered to be statistically significant.

Human study population. The study protocol was approved by all local ethics committees and informed consent was obtained from each subject before participation in the study, in accordance with the Declaration of Helsinki principles. For children younger than 18 years, an oral consent was obtained and parents provided written informed consent. All subjects were of European origin.

Human gene expression analysis. We used liver, subcutaneous and omental adipose tissue samples from the Atlas Biologique de l'Obésité Sévère' (ABOS) cohort (ClinicalGov NCT01129297), a cohort studied in the Département de Chirurgie Générale et Endocrinienne[28] (Lille CHRU). Total RNA was extracted from the tissues using an RNeasy protect Mini Kit (QIAGEN) and quantified by absorbance at 260 nm and 280 nm in a PerkinElmer spectrophotometer. Human *GPR120*, *FABP4*, *PPARG*, *CD68* and *SCD* mRNA levels were quantified by reverse transcription reaction followed by qRT–PCR. Quantitative assessment of human mRNA expression was performed using TaqMan Gene Expression Assays (Hs01111664_m1: *GPR120* and Hs99999905_m1: *GAPDH*; Hs00609791_m1: *FABP4*; Hs00234592_m1: *PPARG*; Hs00154355_m1: *CD68*; Hs01682761_m1: *SCD*; Applied Biosystems) with an Applied Biosystems 7900HT Fast Real-Time PCR System. As an internal control for potential housekeeper reference variability, gene transcript levels were normalized to *GAPDH* reference housekeeper transcript level. The mean of the triplicate cycle thresholds of the target was normalized to the mean of triplicate cycle thresholds of the reference internal housekeeper genes using the formula $2^{CT_{GAPDH} - CT_{target}}$, which yielded a relative target-to-reference transcript concentration value as a fraction of reference transcript. Samples for which the cycle threshold was above 35 were excluded from the analysis.

***GPR120* exon sequencing.** We sequenced the four *GPR120* exons in 312 obese patients including 121 French obese adults and 191 French obese children who were recruited by the CNRS-UMR8199 unit and the Department of Nutrition of Paris Hotel Dieu Hospital. *GPR120* is located on human chromosome 10q23.33 and encodes a 377-amino-acid protein (NCBI NM_181745.3 and NP_859529). PCR conditions and primer sequences are available on request. Fragments were bidirectionally sequenced using the automated 3730xl DNA Analyzer (Applied Biosystems). Electrophoregram reads were assembled and analysed using the VARIANT REPORTER software (Applied Biosystems). The locations of the variants are displayed by base numbers counting from the ATG translation initiation codon following the Human Genome Variation Society nomenclature for the description of sequence variations. The positions of mutations were indicated by reference to the human genome build NCBI36/hg18.

Genotyping of the p.R270H and p.R67C/rs6186610 variants. We genotyped the two non-synonymous variants in 6,942 unrelated obese subjects and in 7,654 control subjects, all of European descent. Genotyped populations are described in Supplementary Table 4. The set of obese subjects included 516 unrelated French obese children who were recruited by the CNRS-UMR8199 unit or Toulouse Children's Hospital[29]; 332 Italian obese children from Verona[30] or Rome[31]; 170 Finnish obese adolescents from the Northern Finland Birth Cohort 1986[32]

(NFBC1986); 1,164 unrelated French obese adults from the ABOS cohort[28] or recruited by the CNRS-UMR8199 unit and the Department of Nutrition of Paris Hotel Dieu Hospital[29]; 2,514 Belgian obese patients from the outpatient obesity clinic at Antwerp University Hospital[33]; 1,736 Swiss obese subjects who were recruited after gastric surgery in Zurich[34]; and 510 Greek obese subjects recruited in the Hippokration Hospital of Thessaloniki or in the Second Department of Internal Medicine of the Hospital of Alexandroupolis[35]. The set of control subjects included 422 Italian lean children from Verona[30]; 4,639 Finnish lean adolescents from the NFBC1986 cohort[32]; 1,976 French lean adults from the D.E.S.I.R (Data from the Epidemiological Study on the Insulin Resistance syndrome) prospective study[36] and from the Haguenau study[37]; 148 Belgian lean subjects from Antwerp Hospital[33]; and 469 Greek lean individuals recruited in medical examination centres in Thessaloniki[35]. The 1,109 French pedigrees selected for obesity were recruited by the CNRS-UMR8199[38], and the 780 German childhood obesity trios were recruited at the Universities of Marburg and Essen[39]. The p.R270H variant was genotyped using the LightCycler 480 High Resolution Melting (HRM) Master kit (Roche), following the manufacturer's protocol. Genotyping of p.R67C/rs6186610 was performed using a custom TaqMan assay according to the manufacturer's instructions (Applied Biosystems). Allelic discrimination was performed using an Applied Biosystems 7900HT Fast Real-Time PCR System and SDS 2.3 software. For both variants, genotype success rate was at least 95% and no deviation ($P > 0.05$) from Hardy–Weinberg equilibrium was observed in any of the examined populations.

Phenotyping. The 90th and 97th body mass index (BMI) percentiles were used as thresholds for childhood overweight and obesity, respectively, according to the recommendations of the European Childhood Obesity Group study in local reference populations[40,41]. Adult subjects were defined as normal (BMI $< 25\,kg\,m^{-2}$), overweight ($25 \leq$ BMI $< 30\,kg\,m^{-2}$) and obese (BMI $\geq 30\,kg\,m^{-2}$) according to the International Obesity Task Force recommendations.

***In silico* analysis of both p.R270H and p.R67C variants.** Phylogenetic conservation of the part of *GPR120* containing each non-synonymous variant was assessed using the UCSC genome browser (Vertebrate Multiz Alignment & Conservation), based on a phylogenetic hidden Markov model, phastCons[42]. To predict the possible effect of both amino-acid substitutions on the structure and function of GPR120, we used several programs: the POLYPHEN (polymorphism phenotyping) web-based program[43,44]; PANTHER[45] (protein analysis through evolutionary relationships); the SIFT (sorting intolerant from tolerant) algorithm[46]; the SNAP (screening for non-acceptable polymorphisms) software[47]; and the PMUT web-based program[48].

Plasmid construction. A FLAG-human GPR120/pcDNA5/FRT/TO plasmid was constructed by ligating GPR120 complementary DNA into the multicloning site of the mammalian expression vector pcDNA5/FRT/TO (Invitrogen) with the amino-terminal FLAG tag. The point mutation for constructing the FLAG-human GPR120 p.R67C/pcDNA5/FRT/TO and FLAG-GPR120 p.R270H/pcDNA5/FRT/TO plasmids was carried out using the following primers: p.R67C (sense: 5′-ggtgctggtggcgtgccgacgacgcc-3′; antisense: 5′-ggcgtcgtcggcacgccaccagcacc-3′) and p.R270H (sense: 5′-agccaccagatccacgtgtcccagcaggac-3′; anti-sense: 5′-gtcctgctggga cacgtggatctggtggct-3′). All constructs were confirmed by DNA sequencing.

Cell lines and cell culture. Flp-In T-REx-293 (T-REx 293) cells (Invitrogen) were used to develop inducible and stable cell lines expressing GPR120 (wild type, p.R270H or p.R67C). T-REx 293 cells were routinely cultured in Dulbecco's modified Eagle's medium (DMEM; Sigma) supplemented with 10% FBS, $100\,\mu g\,ml^{-1}$ Zeocin (Invitrogen) and $10\,\mu g\,ml^{-1}$ blasticidin S (Funakoshi). T-REx 293 cells were transfected with FLAG–GPR120 (wild type, p.R270H or p.R67C)/pcDNA5/FRT/TO using Lipofectamine reagent (Invitrogen) and selected with DMEM, which had been supplemented with 10% FBS, $10\,\mu g\,ml^{-1}$ blasticidin S and $100\,\mu g\,ml^{-1}$ hygromycin B (Gibco BRL). GPR120 protein expression was induced by adding $10\,\mu g\,ml^{-1}$ of doxycycline hyclate (Dox; Sigma) for 48 h. Human NCI-H716 cells were obtained from the American Type Culture Collection (Manassas). Cells were grown in suspension in Roswell Park Memorial Institute 1640 medium supplemented with 10% FBS, $100\,IU\,ml^{-1}$ penicillin and $100\,\mu g\,ml^{-1}$ streptomycin.

$[Ca^{2+}]_i$ response analysis. Cells were seeded at a density of 2×10^5 cells per well on collagen-coated 96-well plates, incubated at 37 °C for 21 h and then incubated in Hanks' Balanced Salt Solution (HBSS, pH 7.4) containing Calcium Assay Kit Component A (Molecular Devices) for 1 h at 20 °C. ALA used in the fluorometric imaging plate reader (FLIPR, Molecular Devices) assay were dissolved in HBSS containing 1% DMSO and prepared in another set of 96-well plates. These plates were set on the FLIPR, and mobilization of $[Ca^{2+}]_i$ evoked by agonists was monitored.

Transfection. One million cells were seeded into a 3.5-cm-diameter dish before transfection. NCI-H716 cells were transfected with 5 μg of each plasmid using Lipofectamine 2000 (Invitrogen) according to the manufacturer's protocol. At 24 h post-transfection, transfection of each FLAG-tagged construct was confirmed by anti-FLAG FACS analysis. Then the cells were reseeded in 24-well culture plates coated with Matrigel matrix (BD Biosciences) at a density of approximately 3×10^5 cells per well for the secretion studies. To test the effect of variant receptors on the ALA-induced $[Ca^{2+}]_i$ response of the wild-type receptor, 2×10^7 T-REx 293 cells expressing Dox-inducible FLAG–GPR120 wild type were seeded into a 15-cm-diameter dish before transfection. Cells were then transfected with 32 μg of each plasmid (empty vector, wild type and p.R270H GPR120) using Lipofectamine 2000 (Invitrogen) according to the manufacturer's protocol. At 24 h post-transfection, cells were reseeded at a density of 2×10^5 cells per well on collagen-coated 96-well plates and treated with $10\,\mu g\,ml^{-1}$ of Dox, and at 48 h post-transfection, ALA-induced $[Ca^{2+}]_i$ response was monitored.

GLP-1 secretion analysis. Cells were serum-starved with FBS-free DMEM for 3 h, washed with HBSS and incubated for 2 h at 37 °C in 0.3 ml FBS-free DMEM containing DMSO (negative control), 1 μM phorbol 12-myristate 13-acetate (positive control) or 100 μM ALA. Supernatants were collected and the active GLP-1 concentration in the supernatant was determined by enzyme immunoassay using GLP-1 (Active) ELISA Kit (Millipore).

Flow cytometry analysis. Anti-FLAG (Sigma) and anti-HA (Roche) antibodies were used for staining. Data were acquired and analysed on FACSCalibur with CELLQUEST software (Becton Dickinson).

Statistical analysis of human study. We assessed the effect of both non-synonymous variants (p.R270H and p.R67C) on obesity using a logistic regression adjusted first for age and gender and then for age, gender and geography, under an additive model, using the software R (version 2.12). Adjustment for geography was achieved to reflect a north–south gradient between the six different countries of origin of the study participants. An ordinal variable was created and coded: 1 for Finland, 2 for Belgium, 3 for France and Switzerland, 4 for Italy and 5 for Greece. This variable was added as a covariate in the logistic regression model.

Data analysis for the $[Ca^{2+}]_i$ response was performed using IGOR PRO (WaveMetrics). Significant differences between expression among wild-type and heterozygous groups, and among lean and obese wild-type subjects, were assessed using non-parametric Mann–Whitney analysis (GRAPHPAD PRISM 5 software).

27. Gautier, L., Cope, L., Bolstad, B. M. & Irizarry, R. A. affy–analysis of Affymetrix GeneChip data at the probe level. *Bioinformatics* **20,** 307–315 (2004).
28. Poulain-Godefroy, O., Lecoeur, C., Pattou, F., Fruhbeck, G. & Froguel, P. Inflammation is associated with a decrease of lipogenic factors in omental fat in women. *Am. J. Physiol. Regul. Integr. Comp. Physiol.* **295,** R1–R7 (2008).
29. Meyre, D. *et al.* Genome-wide association study for early-onset and morbid adult obesity identifies three new risk loci in European populations. *Nature Genet.* **41,** 157–159 (2009).
30. Morandi, A. *et al.* The Q121 variant of ENPP1 may protect from childhood overweight/obesity in the Italian population. *Obesity (Silver Spring)* **17,** 202–206 (2009).
31. Buzzetti, R. *et al.* PPAR-γ2 Pro12Ala variant is associated with greater insulin sensitivity in childhood obesity. *Pediatr. Res.* **57,** 138–140 (2005).
32. Järvelin, M. R. *et al.* Ecological and individual predictors of birthweight in a northern Finland birth cohort 1986. *Paediatr. Perinat. Epidemiol.* **11,** 298–312 (1997).
33. Peeters, A. *et al.* Variants in the FTO gene are associated with common obesity in the Belgian population. *Mol. Genet. Metab.* **93,** 481–484 (2008).
34. Steffen, R., Potoczna, N., Bieri, N. & Horber, F. F. Successful multi-intervention treatment of severe obesity: a 7-year prospective study with 96% follow-up. *Obes. Surg.* **19,** 3–12 (2009).
35. Rouskas, K. *et al.* Association between BBS6/MKKS gene polymorphisms, obesity and metabolic syndrome in the Greek population. *Int. J. Obes. (Lond.)* **32,** 1618–1625 (2008).
36. Balkau, B. An epidemiologic survey from a network of French Health Examination Centres (D.E.S.I.R.): epidemiologic data on the insulin resistance syndrome [in French]. *Rev. Epidemiol. Sante Publique* **44,** 373–375 (1996).
37. Jaquet, D., Collin, D., Levy-Marchal, C. & Czernichow, P. Adult height distribution in subjects born small for gestational age. *Horm. Res.* **62,** 92–96 (2004).
38. Meyre, D. *et al.* R125W coding variant in TBC1D1 confers risk for familial obesity and contributes to linkage on chromosome 4p14 in the French population. *Hum. Mol. Genet.* **17,** 1798–1802 (2008).
39. Jarick, I. *et al.* Novel common copy number variation for early onset extreme obesity on chromosome 11q11 identified by a genome-wide analysis. *Hum. Mol. Genet.* **20,** 840–852 (2011).
40. Poskitt, E. M. Defining childhood obesity: the relative body mass index (BMI). European Childhood Obesity group. *Acta Paediatr.* **84,** 961–963 (1995).
41. Rolland-Cachera, M. F. *et al.* Body mass index variations: centiles from birth to 87 years. *Eur. J. Clin. Nutr.* **45,** 13–21 (1991).
42. Siepel, A. *et al.* Evolutionarily conserved elements in vertebrate, insect, worm, and yeast genomes. *Genome Res.* **15,** 1034–1050 (2005).
43. Ramensky, V., Bork, P. & Sunyaev, S. Human non-synonymous SNPs: server and survey. *Nucleic Acids Res.* **30,** 3894–3900 (2002).
44. Sunyaev, S. *et al.* Prediction of deleterious human alleles. *Hum. Mol. Genet.* **10,** 591–597 (2001).
45. Thomas, P. D. *et al.* PANTHER: a library of protein families and subfamilies indexed by function. *Genome Res.* **13,** 2129–2141 (2003).
46. Kumar, P., Henikoff, S. & Ng, P. C. Predicting the effects of coding non-synonymous variants on protein function using the SIFT algorithm. *Nature Protocols* **4,** 1073–1081 (2009).

47. Bromberg, Y., Yachdav, G. & Rost, B. SNAP predicts effect of mutations on protein function. *Bioinformatics* **24,** 2397–2398 (2008).

48. Ferrer-Costa, C. *et al.* PMUT: a web-based tool for the annotation of pathological mutations on proteins. *Bioinformatics* **21,** 3176–3178 (2005).